Bunch-by-bunch three-dimensional position and charge measurement in a storage ring

Xingyi Xu

Shanghai Institute of Applied Physics, Chinese Academy of Sciences, Shanghai 201800, China
and University of Chinese Academy of Sciences, Beijing 100049, China

Yongbin Leng,[*] Yimei Zhou, Bo Gao, Jian Chen, and Shanshan Cao

Shanghai Advanced Rearch Institute, Chinese Academy of Sciences, Shanghai 201204, China;
Shanghai Institute of Applied Physics, Chinese Academy of Sciences, Shanghai 201800, China;
and University of Chinese Academy of Sciences, Beijing 100049, China

Bunch-by-bunch beam parameters monitor is a very useful tool for accelerator operation and optimization. An *in situ* bunch-by-bunch three-dimensional position and charge measurement system has been developed at the Shanghai Synchrotron Radiation Facility. Signals from beam position monitors carry almost full beam information, a broadband digital receiver can retain most information. Therefore, a four-channel wideband oscilloscope is employed to capture the signals from all electrodes of the beam position monitor. Correlation coefficient-based methods are used to extract these bunch-by-bunch parameters synchronously. We evaluated the performance of this bunch-by-bunch information extraction method, the measurement uncertainty of longitudinal phase is less than 0.2 ps, the uncertainty of transverse position is less than 10 μm and the charge uncertainty is 0.3% under the condition that the bunch charge is 600 pC. Thanks to the great performance of the new system, it is accurate enough to study the transient state during injection. In addition, an *in situ* wakefield measurement system is planned to be established based on this system.

I. INTRODUCTION

Brightness and stability are key specifications of the third-generation synchrotron radiation light sources [1], which have the following basic characteristics: ultra-low beam emittance (few nmrad or even tens of pmrad), ultrahigh beam stability(orbital feedback control accuracy is mostly micron or submicron level), high average beam current (above 300 mA), small-aperture beam vacuum pipe (below 30 mm in diameter), a large number of vacuum inserts, top-up operation mode, small dynamics aperture, with high time resolution experiment ability (time resolution ps order) and so on [2]. The above-mentioned characteristics make the following scientific and technological problems the focus of research and solution: how to ensure beam stability under the condition of large current intensity and how to minimize the disturbance of the injection process to users.

In order to increase the instability threshold of the charge of each bunch, high-order harmonic cavity technology is usually used to increase the charge of each bunch through the longitudinal bunch distribution control of multiple high frequency systems, thereby increasing the total average current. It is necessary to carry out online synchronous monitoring of the transverse and longitudinal parameters of each bunch to determine how the amplitude and phase parameters of these high-frequency systems work together best. At the same time, it is also necessary to design and develop a bunch-by-bunch feedback system with reasonable bunch-by-bunch parameters to suppress the instability of the beam in the operation process to ensure the regular operation. In addition, "top-up" operation mode requires frequent injection to maintain a constant high current. The injection process is a disturbance for the storage ring, which will affect the beam stability. It is significant to obtain real-time bunch-by-bunch three-dimensional parameters including the position and size parameters of both stored and injected bunches to optimize the injector and kickers parameters.

On the other hand, although the regular injection process (about once every 10 minutes for Shanghai Synchrotron Radiation Facility) is a disturbance for user's experiments, it provides an opportunity for accelerator physicists and

beam diagnostic personnel to monitor machine status in real time and obtain more beam information [3–5]. The storage ring is very stable during decay mode, transverse oscillation amplitude is usually suppressed to a few microns, longitudinal oscillation amplitude is usually suppressed to a few picoseconds, and the closed-orbit stability reaches submicron. Most of beam parameters that can be measured are steady-state (such as current, closed-orbit, bunch length, profile size). If no excitation (disturbance) is applied, more machine parameters (such as Beta function, chromaticity, damping time, instability growth time) cannot be obtained. It is difficult to judge whether the synchrotron radiation facility is operating under the design model and whether there is operating risk. If the three-dimensional parameters of the bunches can be monitored in real time of each inject events, it is possible to obtain the above-mentioned machine parameters through the analysis of this unsteady state process, so as to realize the online tracking of the machine status and even the early warning of operational risks.

Obviously, it is necessary to establish a bunch-by-bunch parameter measurement system with high resolution and high refresh rate. In the early days, limited by electronics technology, beam measurement generally performed on the storage ring mainly included beam closed-track measurement [6] and turn-by-turn beam measurement [7]. In recent years, with the development of electronic technology and the need for accelerator machine research, high-precision bunch-by-bunch measurement has become a hot spot in accelerator research around the world [8,9,9–22].

The bunch-by-bunch measurement mainly includes transverse position measurement, longitudinal phase measurement and charge measurement. High-resolution transverse position measurement is most important for studying the three-dimensional bunch position movement process. The commonly used measurement methods mainly include three categories: bunch-by-bunch measurement based on commercial bunch-by-bunch feedback system, bunch-by-bunch measurement system based on digital oscilloscope, and bunch-by-bunch measurement system based on high-speed acquisition board. Among them, the additional function provided by the commercial bunch-by-bunch transverse feedback system is the earliest method used for bunch-by-bunch position measurement. Commonly used commercial processors include the digital feedback processor designed by Spring-8 [23] and commissioned by TED (Tokyo Electron Device), the Libera BXB module (bunch-by-bunch unit) developed by I-tech [24], and the iGp (Integrated Gigasample Processor) BXB feedback processor by Dimtel [25]. Bunch-by-bunch transverse feedback systems have been widely used in electron storage rings, such as ALS [26], PEP-II [27], DAΦNE [28], DELTA [29], TLS [30], DIAMOND [31], ANKA [32], BEPC-II [33], HLS [34], etc. Some laboratories have specially developed bunch-by-bunch measurement systems based on high-speed acquisition boards, which not only

realizes the measurement of important bunch parameters, but also can be used for beam dynamics analysis, injection transient process and research on unstable phenomena such as beam loss. In addition, institutions such as SSRF [15] and PLS [35] used oscilloscopes to measure the transverse position of each bunch.

Longitudinal phase measurement (sometimes called beam arrival time measurement in free electron lasers) is another key part of bunch-by-bunch measurement. The accelerator facilities are usually equipped with a bunch-by-bunch longitudinal feedback system to solve problems such as longitudinal instability. The longitudinal feedback system of most accelerators is based on I-techs Libera bunch-by-bunch module and Dimtels iGp bunch-by-bunch feedback processor [36–39]. In addition to feedback system, the most common method is using an oscilloscope for direct measurement, such as LNLS [40], NSLS-II [41], Spring-8 [42] and so on. Considering data acquisition and online applications, most devices will also use phase detectors or IQ detections to achieve longitudinal phase measurement, such as KEK-PF [43], NSLS-II [41], etc. KEKB has proposed a set of bunch-by-bunch detection method based on the gate circuit [44,45].

Bunch-by-bunch charge measurement is an indispensable part of bunch-by-bunch measurement. For synchrotron radiation facilities, the BCM (beam current monitor) system is an important beam measurement subsystem for monitoring the beam filling mode and studying the operating status of the machine. The front-end signal pickup of the BCM system usually includes BPM, synchrotron radiation light, fast current transformer (FCT) and wall current probe (WCM), etc. The commonly used signal acquisition equipment are digital beam signal processors and oscilloscopes. The former is widely used in NSLS-II [46], BEPC-II [47], SSRF [48], and ALS [49]. The latter is used in Australian Synchrotron [50], Swiss Light Source [51], HLS [52] and other facilities. The most representative ones are the work of ALS and HLS in recent years. ALS has upgraded the BCM system in recent years, subdividing the length of the ALS loop into 62.5 ps (twice the beam length) interval, changing the sampling position by setting timeshift, and finally covering the entire sampling loop. After summing all the sampling points, use DCCT to calibrate the charge of each bunch. The storage ring charge measurement accuracy of this system is better than 1%, and the beam loss of 0.2 pC can be measured. Unlike this, HLS presents a novel bunch current measurement system based on monitoring the distribution of synchrotron radiation. According to preliminary tests of the daily operation mode and single-bunch mode, the measured root-mean-square of the beam current is 1%.

In summary, research institutions around the world have put forward many excellent solutions for bunch-by-bunch measurement. However, it can be seen that for the existing bunch-by-bunch measurement system, the measurement of

the transverse position, longitudinal phase and charge is relatively independent. Each subsystem is composed of different hardware and software from signal pick-up to signal processor. According to the survey results, there is almost no mature bunch-by-bunch three-dimensional position and charge measurement system. It is also very meaningful to measure each parameter independently, but for the study of some physical processes, simultaneously measurement is necessary.

This paper reports the new progress in the bunch-by-bunch three-dimensional position and charge measurement. We have developed a set of signal processing methods based on correlation functions and software resampling, beam parameters can be measured with high repetition rate from the button beam position monitor (BPM). Using this system, the three-dimensional position and charge of all bunches on every turn can be measured simultaneously. The measurement uncertainty of the system is evaluated. Without external clock and complex electronics front-end, the measurement uncertainty of the method is improved compared with the traditional amplitude difference ratio and algorithm.

II. THEORETICAL BASIS

Figure 1 shows cross section (left) and longitudinal section (right) of a button BPM. When a bunch passes through the button electrode, the electrical signal will be drawn from the electrode by the feedthrough, which contains almost all parameter information of the bunch. In the following analysis, we consider N particles of charge e in a bunch of root-mean-square temporal length α (in time units). A bunch with a longitudinal Gaussian distribution can be expressed in the time domain as following [53,54]:

$$I_0 = \frac{eN}{\sqrt{2\pi}\alpha}\exp\left(-\frac{(t-t_0)^2}{2\alpha^2}\right). \tag{1}$$

Where t_0 is the time interval relative to the reference time. When a bunch passes through the electrode, due to electrostatic induction, induced charges $Q(t)$ will accumulate on the electrode:

$$Q(t) = I_0(t) \cdot f(\text{area}) \cdot F(\delta,\theta). \tag{2}$$

$f(\text{area})$ is a factor of the electrode area, which is related to the shape and size of the electrode normal plane. where the position related equation has been derived in [11]:

$$F(\delta,\theta) = \frac{a^2 - \delta^2}{a^2 + \delta^2 - 2a\delta\cos\theta}. \tag{3}$$

$$\delta = \sqrt{x^2 + y^2}. \tag{4}$$

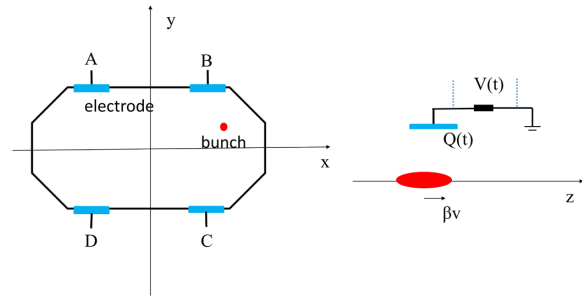$$\theta_{A,B,C,D} = \frac{m\pi}{4} - \tan^{-1}\left(\frac{y}{x}\right) \quad (m = 3, 1, 7, 5). \tag{5}$$

FIG. 1. Cross section (left) and longitudinal section (right) of button-type BPM.

When the external resistance is Z, the signal $V(t)$ we can collect is

$$V(t) = I(t) \cdot Z$$
$$= \frac{-Z}{\beta c} \cdot \frac{t-t_0}{\alpha^2} \cdot I_0(t) \cdot f(\text{area}) \cdot F(\delta,\theta). \tag{6}$$

Where I(t) is the current intensity through the resistor. It can be seen from Eq. (6) and Eq. (1) that the collected voltage signal is related to the transverse position($F(\delta,\theta)$), longitudinal position(longitudinal phase t_0) and charge($e \cdot N$) of bunch. Therefore, there is theoretical support for extracting bunch-by-bunch parameters from the signal.

Unfortunately, the actual collected signal is not completely in accordance with the theoretical derivation, the limited bandwidth of the feedthrough will introduce time delays. In addition, the bandwidth limitation of the acquisition device will also change the signal waveform in the time domain. Therefore, we have done a lot of algorithmic work to try to extract the bunch-by-bunch parameters from the time domain signal.

III. PARAMETERS EXTRACTION ALGORITHM

The signal excited by a bunch passing through the BPM collected by a broadband device is very short-lived (about 1 ns on SSRF), which means that the acquisition device can only collect a small number of sampling points. As shown in Fig. 2, it is the signal we obtain when each bunch passing BPM under regular operation (top-up). The signal is actually several points on the continuous smooth response function:

$$S(t_0, n) = \text{Func}\left(t_0 + \frac{n-1}{f}\right) \quad (n = 1, 2\ldots). \tag{7}$$

Where t_0 is the time of the 1th sampling point relative to the reference instant. n is sampling point index. $S(t_0, n)$ is sampling point value. Func(t) is response function which represents signal excited by a bunch passing a button electrode. f is the sampling frequency. It can be known from Eq. (6) and Eq. (1) that the shape of the response function is mainly affected by the bunch length. Since the bunch status
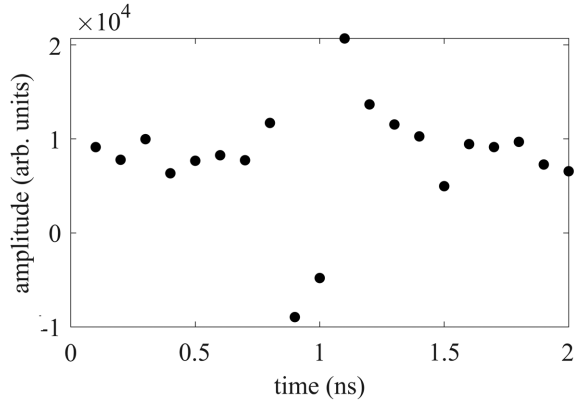
FIG. 2. The signal obtained when a bunch passes BPM. The rf frequency is about 499.654 MHz and the sampling frequency is 10 GHz.

in the storage ring is relatively stable, the charge distribution of the bunch can be considered unchanged on the order of milliseconds. Therefore, the response function is constant within milliseconds. The following formula holds:

$$f \neq m \cdot f_c. \tag{8}$$

m is the positive integer. When the bunch passes through the BPM again, the acquire signal point will not be in the same position of the response function last time. f_c is the revolution frequency. t_0 can be obtain when the bunch passes the BPM every turn, because f_c and f are known. On the basis of removing the initial phase t_0, through the splicing of multiturn sampling data, a high sampling rate response function (about 100 THz for us) is constructed. Because of the different charge distributions, the response functions of different bunches are different. The response function for each bunch is constructed separately. I construct the response function separately for each button and each bunch. The shape of each electrode and the connected cable cannot be guaranteed to be exactly the same. This means that the response function of each channel will not be exactly the same. Therefore, independent construction of the response function is a better choice.

Due to the signal noise and the oscillation of the transverse position of the bunch, the high sampling rate response function constructed by multiturn splicing is not very smooth. In addition to betatron oscillation, ADC sampling error, longitudinal phase oscillation will cause turn-by-turn variation, too. To eliminate the turn-by-turn variation, "window smoothing" comes in. The response function is the most probable distribution of data in different turn. From a mathematical point of view, the turn-by-turn variation can be almost completely eliminated by window smoothing. Based on the minimum sum of Euclidean distances from nearby sampling points, we obtained the smooth response function with less noise and lower sampling rate (about 10 THz).

In detail, the splicing of the response function is a combination of thousands of discrete signals excited when the same bunch passes through the BPM electrode thousands of times. The revolution frequency (f_c) and the sampling frequency of the oscilloscope (f) are accurately known (the uncertainty is less than 100 fs), which means that this splicing can be done through mathematical calculations. After finding the signal of the same bunch on each turn, the position of the signal on absolute time axis is calculated. After the phase alignment is completed, these signals constitute the initial response function of the bunch. Due to the inconsistency of sampling (mainly from the ADC of the acquisition device, longitudinal phase jitter, and transverse position jitter), the response function obtained by direct splicing of measurement data will not be very smooth. However, ADC sampling error, phase jitter, and position jitter are all evenly distributed, so the fine response function is the most probable value of the response function obtained by splicing. By window smoothing the initial response function, the fine response function represented by its most probable distribution is obtained. In order to save computing resources, the fine response function after window smoothing is resampled by software to obtain a standard response function with a lower equivalent sampling rate for subsequent data processing. Figure 3 shows the construction result of the response function of a sample bunch. We selected the data during the injection process to construct the response function. During this time, the betatron oscillation is the strongest in the regular operation of SSRF. It can be seen that the algorithm still works well if the beam is undergoing betatron oscillation.

It is feasible to obtain the response function with a stable beam and reuse it for other measurements. But this is not the best choice. Building the response function in real time will be better. It can be known from Eq. (6) and Eq. (1) that the shape of the response function is mainly affected by the bunch length. If the beam length changes in different
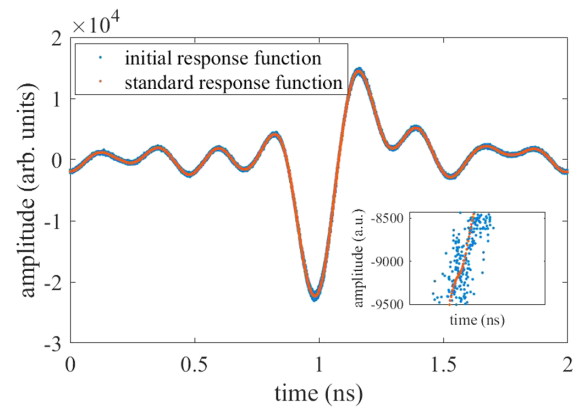

FIG. 3. The initial response function(red) and standard response function(blue) of a typical bunch when the beam is undergoing betatron oscillation.

experiments, using the response function constructed with a stable beam (different bunch length) will cause the measurement resolution to decrease.

It can been seen from Fig. 3 that the bunch signal contains ringing signal. Most of the ringing signal is part of the single bunch signal and not from the leading bunches. The bandwidth is not infinite and the cable has lead resistance, lead inductance, and stray capacitance, the ringing signal is generated. This is a valid signal, and the ringing signal also contains amplitude and phase information. At high bandwidth, the first bunch and the last bunch in a bunch train have similar response functions. Therefore, the influence of the ringing signal on the measurement is limited. In addition, in each measurement, the response function is established in real time, and even if there is a limited ringing signal from the leading bunches, this part of the signal is also included in the establishment of the response function. In other words, we do not start the fitting of the bunch shape with pure single bunch response. It will not have a great impact on the bunch measurement.

Bunch-by-bunch longitudinal phase consists of three parts:

$$\varphi_l = \varphi_{t_0} + \varphi_r + \varphi_c. \tag{9}$$

Where φ_{t_0} is the phase of the first sampling point of the signal acquired when a bunch passes BPM each turn, that is, the initial phase relative to the reference instant. φ_{t_0} is easy to determine. In the case of knowing the index of the starting point of the signal in the whole data, it only depends on the sampling period of the signal acquisition device and the revolution time. φ_r is the phase of response function, it represents the equilibrium phase of a bunch. For different bunch, φ_r is different, because the longitudinal equilibrium phase of each bunch is different. In a physical sense, φ_r represents the equilibrium position of the longitudinal oscillation of the bunch shown in Fig. 4. φ_c is the phase difference relative to the response function. For different bunches and different turns, φ_c is different, and it is the most important part of bunch-by-bunch measurement. We developed a vector-comparison-method based on correlation coefficient to calculate it by comparing the data acquired every time when the bunch passes BPM with the response function of the bunch.

$\mathrm{Func}_m(t)$ is the constructed response function of mth bunch which consists of three parts:

$$\mathrm{Func}_m(t) = \mathrm{Func}_{m_0}(t) + \sum_{i=1, i \neq m}^{N} e_{i,m}(t) + b. \tag{10}$$

Where $\mathrm{Func}_{m_0}(t)$ is the signal excited by bunch m self. b is the baseline which mainly depends on the acquisition equipment. N is the total number of bunch. $e_{i,m}$ is the signal generated by the bunch i at the bunch m which is mainly caused by crosstalk and reflection. $\{d_n^{m,j}\}$ is the data
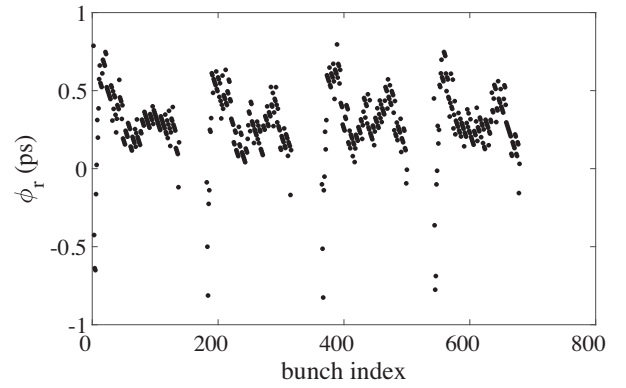

FIG. 4. The equilibrium longitudinal phase(φ_r) of bunches in top-up filling pattern. There are 720 buckets in SSRF.

acquired when bunch m passes the BPM in turn j. $\{d_n^{m,j}\}$ is an array in mathematics.

$$\{d_n^{m,j}\} = k_{m,j} \cdot \mathrm{Func}_{m_0}\left(t_0 + \frac{n}{f}\right)$$
$$+ \sum_{i=1, i \neq m}^{N} k_{i,j} \cdot e_{i,m,j}\left(t_0 + \frac{n}{f}\right) + b$$
$$(n = 1, 2, 3 \ldots). \tag{11}$$

Where $\{d_n^{m,j}\}$ is the array, k is amplitude of signal. For different bunches and different turns, k is different. According to Eq. (6) and Eq. (1), it is proportional to the distance of the bunch from the BPM electrodes and charge of the bunch in the case of ignoring the high-order term. Broadband acquisition equipment ensures that crosstalk is small enough to be ignored. After subtracting the baseline and ignoring $e_{i,m}$ and $e_{i,m,j}$, Eq. (10) and Eq. (11) is simplified to:

$$\mathrm{Func}_m(t) = \mathrm{Func}_{m_0}(t). \tag{12}$$

$$\{d_n^{m,j}\} = k_{m,j} \cdot \mathrm{Func}_{m_0}\left(t_0 + \frac{n}{f}\right). \tag{13}$$

The lookup table ($\{\mathrm{LUT}_n^i\}$) is obtained by software resampling to the response function [$\mathrm{Func}_m(t)$]. The sampling frequency is f(same as the acquisition equipment). The initial phase of the lookup table is t_i.

$$\{\mathrm{LUT}_n^{m,i}\} = \mathrm{Func}_m\left(t_i + \frac{n}{f}\right)$$
$$= \mathrm{Func}_{m_0}\left(t_i + \frac{n}{f}\right) \qquad (n = 1, 2, 3 \ldots). \tag{14}$$

if $t_i = t_0$:

$$\{d_n^{m,j}\} = k_{m,j} \cdot \{\mathrm{LUT}_n^{m,i}\} \qquad (n = 1, 2, 3 \ldots). \tag{15}$$

Mathematically, when $t_i = t_0$, the two arrays are in direct proportion. It means that the two vectors are in the same
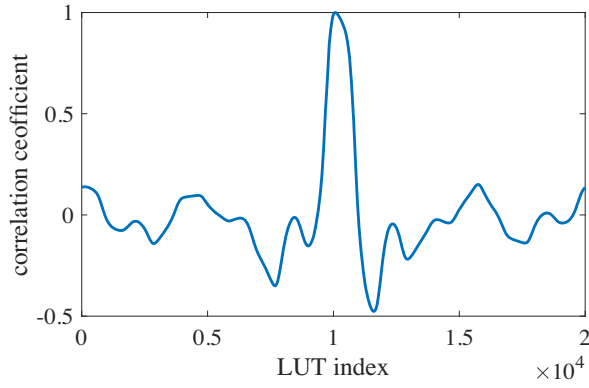
FIG. 5. The relationship between correlation_coefficient and index of LUT. The peak value is close to 1, which indicates that the match is successful and effective.

FIG. 6. Linear fitting of $\{LUT_n^{m,i}\}$ and $\{d_n^{m,j}\}$. $k_{m,j}$ is the slope obtained by fitting.

direction. By finding the lookup table with the closest direction, t_0 can be obtained. A vector-matching-method based on correlation coefficient has been developed to find the lookup table with the closest direction.

$$correlation\_coefficient_{m,j,i} = \cos(\theta)$$
$$= \frac{\mathbf{d_n^{m,j}} \cdot \mathbf{LUT_n^{m,i}}}{|\mathbf{d^{m,j}}| \cdot |\mathbf{LUT^{m,i}}|}. \quad (16)$$

Where correlation_coefficient$_{m,j,i}$ is the correlation coefficient of bunch m in jth turn's data comparing with ith LUT of bunch m. Mathematically, it represents the cosine of the angle between two vectors, ranging from -1 to 1.

$$i_{\text{best}_{m,j}} = \text{argmax}_i(correlation\_coefficient_{m,j,i}). \quad (17)$$

According to Eq. (17), the index of the most matching LUT can be obtained by looking for the maximum value of correlation_coefficient$_{m,j,i}$. Where $i_{\text{best}_{m,j}}$ is the most matching index of bunch m in jth turn. The relationship between correlation_coefficient and index of LUT is shown in Fig. 5.

According to Eq. (15), $k_{m,j}$ can be obtained by linear fitting $\{LUT_n^{m,i}\}$ and $\{d_n^{m,j}\}$. An example of the fitting is
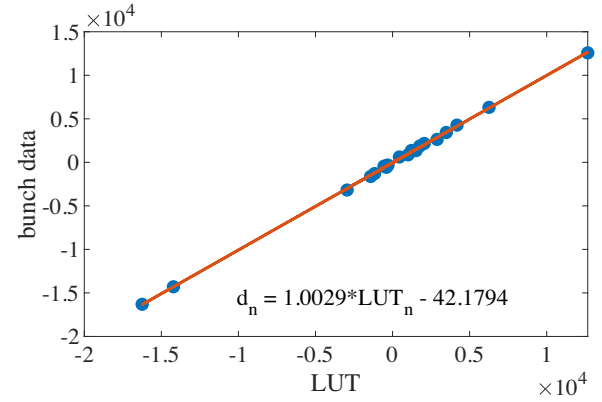
shown in Fig. 6. Bunch-by-bunch transverse position (x,y) and charge (Q) are given as follow:

$$x = k_x \cdot \frac{k_A - k_B - k_C + k_D}{k_A + k_B + k_C + k_D}$$
$$y = k_y \cdot \frac{k_A + k_B - k_C - k_D}{k_A + k_B + k_C + k_D}. \quad (18)$$

Wherein: k_x and k_y are constant. Equation (18) is valid only when the beam is at the center of the vacuum chamber. For offset beam, it includes systematic error. In regular operation of SSRF, the beam is very close to the center of the vacuum chamber, so this algorithm can meet the accuracy requirements. It should be implemented to include polynomial fit to reproduce the monitor chamber structure if the beam is far from the center of the vacuum chamber [55,56].

$$Q = k_q \cdot (k_A + k_B + k_C + k_D). \quad (19)$$

Wherein: k_q is constant.

IV. MEASUREMENT APPARATUS

In order to reduce signal loss, broadband acquisition equipment is necessary. Since there were few standard
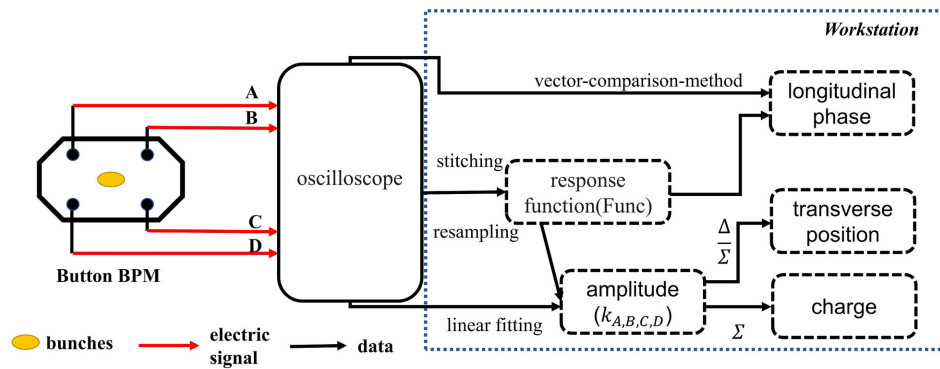

FIG. 7. Measurement scheme and algorithm flow. The oscilloscope direct samples the signal from the BPMs electrodes and fetches the original waveforms over 7000 turns and more than 500 bunches for once. Data processing based on Numba and Python is done in a workstation.

TABLE I. Parameters of SSRF.

Parameter	Value
energy (E)	3.5 GeV
current (I_0)	220 mA
rf frequency (f_{rf})	499.654 MHz
rf cavity voltage (V_{rf})	4.5 MV
buckets (h)	720
revolution frequency (f_o)	694 kHz
bunch length (σ)	18 ps

FIG. 8. The bunch response function with DC-1 GHz bandwidth. The crosstalk between bunches is very large.

electronics that could measure the beam signals with both high sampling rate and huge memory capacity to store the data, a broadband oscilloscope with a 20 GHz maximum sampling rate and 6 GHz analog bandwidth was chosen to record the signals from the four buttons of a BPM owing to its high-sampling rate and available memory capacity (7000 turns of the SSRF operating mode). A workstation is used to extract bunch-by-bunch three-dimensional position and charge from the signals, as shown in Fig. 7. The sampling rate of the oscilloscope was not an integer multiple of the rf frequency (499.654 MHz in our storage ring). As a result, a high sampling rate response function can be obtained by the splicing of multiturn sampling data.

SSRF is a third generation synchrotron radiation light source. It is composed of a group of accelerators: a 150 MeV linear accelerator, a 180 m-long 3.5 GeV booster, and a 432 m long 3.5 GeV storage ring. The machine runs routinely in top-up mode. Four bunch trains, each has 125 consecutive bunches, are evenly spread in the 720 buckets in the storage ring. The relevant parameters of the machine are listed in Table I.

For SSRF, the bunch length is stable at about 18 ps for a long time, and the beam life is several hours, which makes the response function not change in a short time. When the oscilloscope works with four channels, the maximum sampling rate is 10 GHz, that is to say, each channel can get 20 data points from a electrode during the 2 ns time when the bunch passing BPM.

The bandwidth of the system described in this paper is DC-6 GHz, which is much higher than other bunch-by-bunch measurement systems. However, very high bandwidth will introduce no HOM-related components. According to the introduction before, most measurement systems process narrowband signals. Bandwidth is often less than 1 GHz. Although there is no HOM-related components from far place with less than 1 GHz bandwidth, the crosstalk between bunches is very large, which is the reason why most systems cannot achieve strict bunch-by-bunch measurement. In order to evaluate the pros and cons, a special machine experiment was done in SSRF. After setting the bandwidth to DC-1 GHz, we used the same device to construct a single-bunch response function (shown in Fig. 8). It can be seen that the effective range of the response function is longer than 2 ns. The bunch
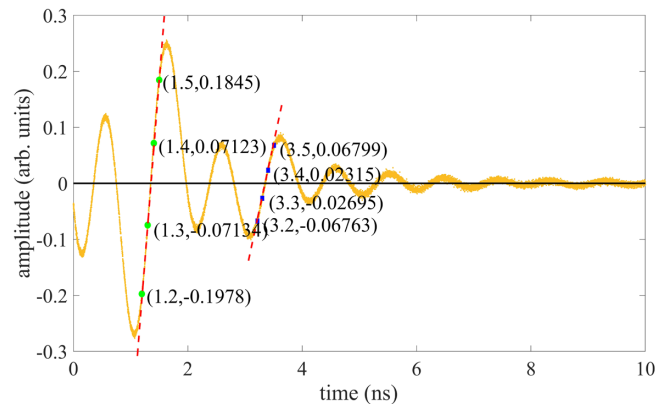
interval is about 2 ns in SSRF. Based on this calculation, the signal crosstalk between the bunches is about 37% with low-pass filter, which is far greater than the influence of HOM-related components. With the high-bandwidth oscilloscope, it not only retains more signal power but also avoids the crosstalk between the bunches, which makes it possible to measure bunch-by-bunch position and charge on every turn. In this case, the post-ringing signal will almost decay to zero before the next bunch signal arrives.

Therefore, although the system bandwidth is higher than the cutoff frequency which will introduces HOM-related components, the bunch data has been measured without low-pass filter.

V. EXPERIMENTS RESULTS

We use this bunch-by-bunch three-dimensional position and charge measurement system to monitor the beam state in SSRF. The experiment does not need special configurations of the machine, so the data were collected unnoticed during daily operations. The typical results plotted in this section were processed by using the data recorded during the injection on July 24, 2020 unless otherwise noted. The reason why we choose the injection process is that the beam has strong betatron oscillations during the injection transient which the influence of kickers.

In one time, the signal recorded by the oscilloscope can be processed to obtain the three-dimensional position and charge of more than 500 bunches in 7000 turns (every turn in 1 ms). The processing time window size is mainly limited by the memory capacity of the oscilloscope. A set of typical results is shown in Fig. 9. After summing the relative charge of all bunches, we use DCCT to calibrate the charge of each bunch. By averaging the charge of bunches in different turns, the filling pattern of the storage ring can be obtained, as shown in Fig. 10.

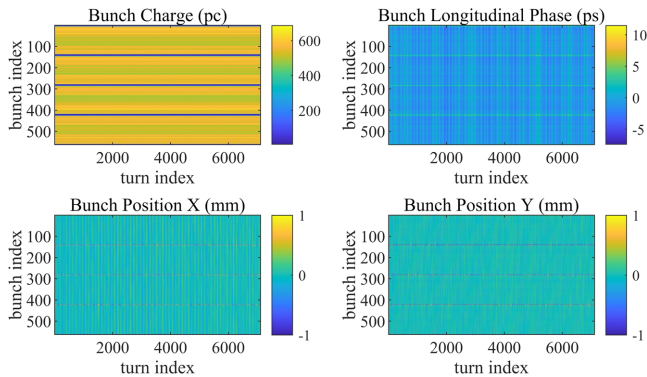The bunch-by-bunch three-dimensional measurement system was used to study the bunch transverse motion

FIG. 9.   Bunch-by-bunch three-dimensional position and charge result.

during injection transient. With signal triggering, we make the injection process happen about 800 turns after the start of the signal acquisition. The transverse position changes of three representative bunches are shown in Fig. 11.

The transverse positions of the bunches before the injection process are very stable. After the injection transient occurs, bunches deviate from the equilibrium position and undergo strong betatron oscillation. The amplitude of transverse oscillation is an exponential decay, it could be considered as a betatron damping oscillation invoked exclusively by the kickers mainly (shown in bunch 300 of Fig. 11). The spatial vector indicated that the kickers fields influencing the bunches were not constant. for bunch 1, this effect of kickers is very small. Therefore, the change of the transverse oscillation amplitude of bunch 1 is mainly affected by the wakefield. The wakefield oscillation of a bunch is determined by the betatron oscillations of all bunches. The propagation coefficient of the wakefield is considered a constant once the drive bunch and the witness bunch are decided, so the amplitude of second mode of a bunch is a linear combination of the amplitudes of the first modes of all bunches (including itself). Bunch 160 is a manifestation of the combined effect of betatron damping oscillation and wakefield oscillation. The PCA method can decompose these multiple coupled motions [18].
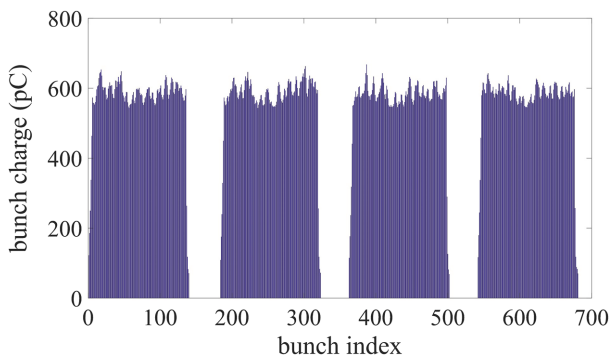

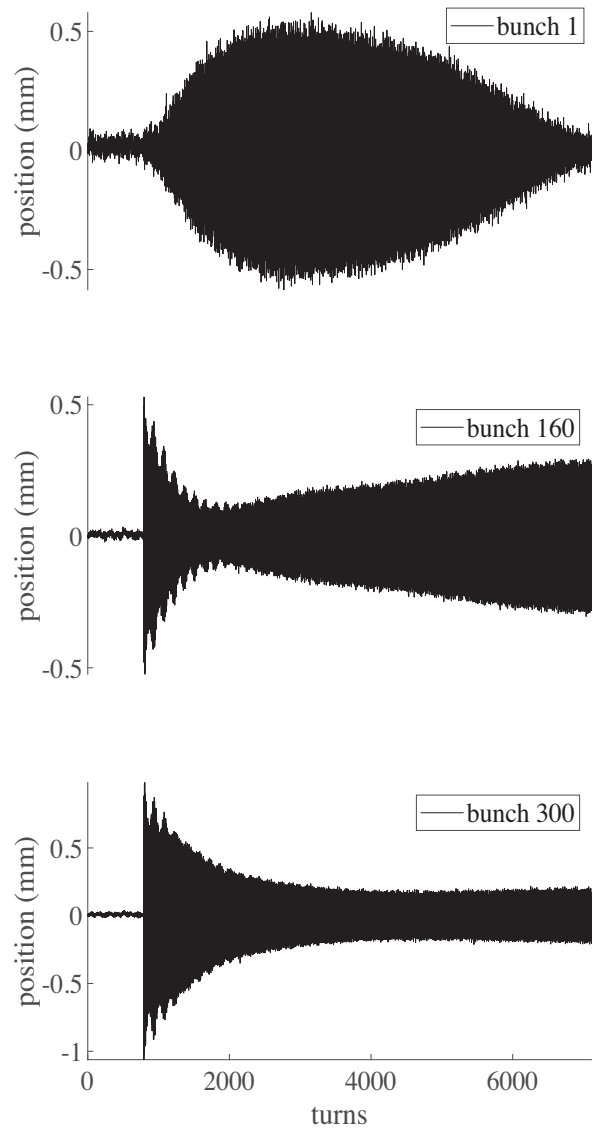FIG. 10.   The filling pattern obtained by averaging bunch-by-bunch charge.

FIG. 11.   The transverse position changes of three representative bunches during injection transient.

The bunch-by-bunch longitudinal phase on every turn is calculated. The bunches have their own longitudinal oscillations in the non-injected state and the frequency of the oscillations is slow. It can be considered that all bunches have an approximately the same common mode oscillation. Figure 12 shows the phase oscillation of multiple stored bunches in the regular operation mode. It can be seen from the figure that the oscillation frequency and amplitude of each bunch are basically the same, but the initial phase is different.

During the injection process, the injector replenishes a small charge on stored bunch. According to the longitudinal phase theory, this refilled charge should behave as a synchronous oscillation. From the measurement results, only superposition with the stored charge can be seen. In this regard, our research group conducted a similar
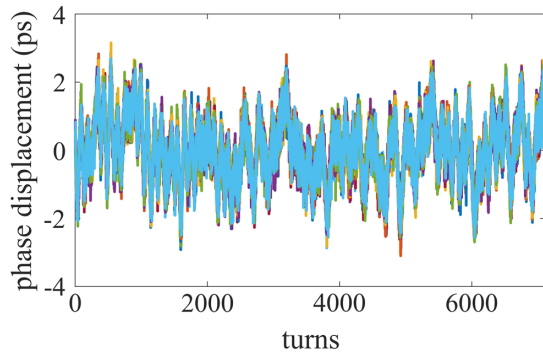
FIG. 12.   Longitudinal phase oscillation of dozens of stored bunches under regular operation mode.

experiment in SSRF [20]. This is not the focus of this paper, so I will not go into details here.

VI. PERFORMANCE EVALUATION

The measurement uncertainty is the most important index of the beam diagnostic system. The following will analyze the measurement uncertainty of charge (current), transverse position, and longitudinal phase. As a necessary condition for the stable work of a synchrotron radiation facility, the charge of bunches is constant in a short time. Therefore, BI (beam instrument) researchers generally use the mean square error of the short-term continuous measured charge as an indicator of measurement uncertainty. The system can measure the charge of all bunches on every turn (694 kHz). The continuous measurement results of a typical bunch are shown in Fig. 13.

The charge of all bunches on every turn is of greater significance to particle physics researchers, and the operators of synchrotron radiation facility are more concerned about the current intensity (average charge of charge). By doing a weighted average of the charges of all bunches in the storage ring, the average charge is obtained (shown in Fig. 14).

The mean square error is used to evaluate the bunch-by-bunch charge measurement uncertainty and the
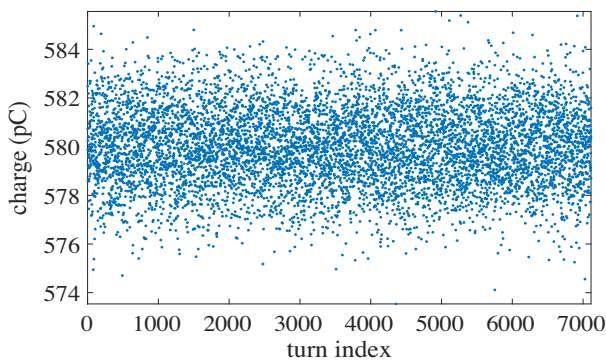
measurement uncertainty of the average charge (current intensity). At a repetition frequency of 694 kHz, for a 600 pC bunch, the uncertainty of bunch-by-bunch charge is 1.6 pC. The uncertainty is better than 0.3%. Under the same conditions, the uncertainty of the average charge (current) measurement is 0.15 pC, which is better than 0.027%.

The PCA method is used to evaluate the resolution of the bunch-by-bunch transverse position and longitudinal phase measurement in this paper. Principal component analysis (PCA) is a commonly used data processing method in the accelerator field. It mainly uses the singular value decomposition (SVD) method to separate correlated signals and random noise, analyzing the signal components in different physical motion modes according to the motion characteristics of the bunches in the accelerator. Compared with traditional processing methods, it can reduce random measurement errors and also remove some systematic measurement errors. In the field of accelerator beam measurement, it is usually used to extract the parameters of the optical model of the storage ring [57,58], the performance evaluation of beam position probes [59], the betatron oscillation phase analysis between beam position probes [60], etc.

For an $m \cdot n$ real number matrix A, it can be decomposed into the following three matrix products:

$$A = USV^T. \qquad (20)$$

U, S, and V are the temporal vectors [57], singular matrix and spatial vectors, respectively. The S matrix only has values on the diagonal, which are usually non-negative real numbers arranged in decreasing order of magnitude. These values are called singular values.

When the singular value is larger, the corresponding principal component is the main common physical mode of the signal. Therefore, the beam motion state can be analyzed according to the signal characteristics of these modes. For beam position measurement, the PCA method is used to decompose the data matrix composed of multiple electrode signals, and the signals related to the main oscillation can be separated separately. The mode with a singular value close to 0 is mainly a vector caused by
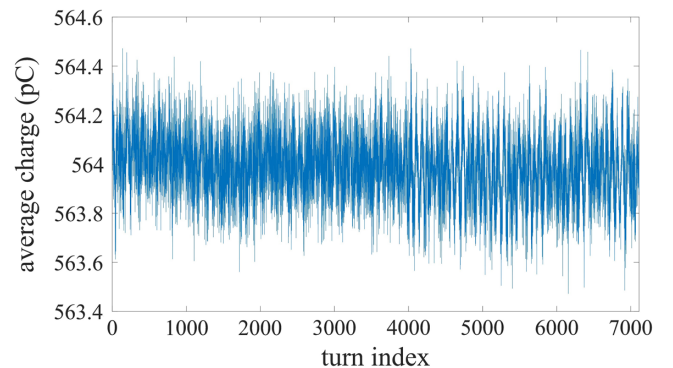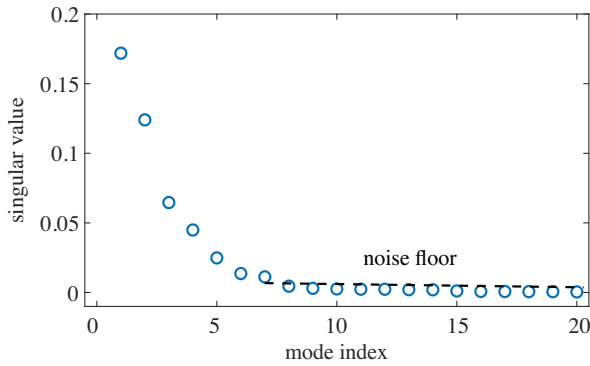

FIG. 13.   The continuous measurement results of a typical bunch.

FIG. 14.   The average charge in different turns.

FIG. 15. The singular values of each transverse position mode obtained by PCA analysis.

FIG. 17. The frequency spectrum analysis of these seven principal components show that they are the betatron oscillations and coupled motions in the vertical and horizontal directions.

various random noises. If the singular values representing the main beam motion mode in the S matrix are also set to 0 and the recombined matrix is denoted as S_1, the result of US_1V^T represents the random noise after beam movement is removed. Calculating the standard deviation of the column vector of this data matrix, you can get the measurement uncertainty of different bunches. Therefore, this method is often used for the resolution evaluation of beam transverse position and longitudinal phase measurement.

The PCA method is used in the uncertainty analysis of the bunch-by-bunch transverse position measurement. The data matrix of the transverse position of 512 bunches on 7000 turns is the real number matrix A, that is, $m = 512$, $n = 7000$. Doing model decomposition in time and space, singular matrix is obtained (shown in Fig. 15).

The first seven principal components (shown in Fig. 16) are the betatron oscillations and their coupled motions in
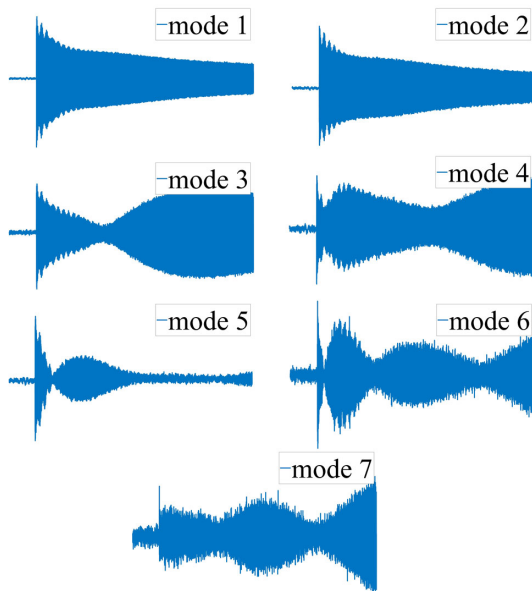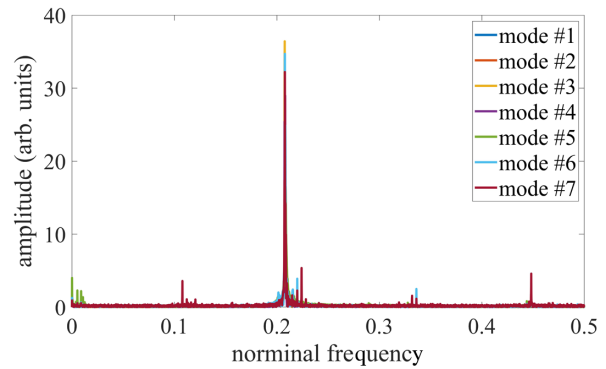
the vertical and horizontal directions, which are the common motion modes of all bunches [18]. The frequency spectrum analysis of these seven motion modes (shown in Fig. 17) shows that the frequency spectrum is consistent with the tune.

According to the above theory, the equation US_1V^T was used to calculate the measurement uncertainty(shown in Fig. 18). The figure shows the transverse position measurement uncertainty of bunches with different charges in the unstable state during the injection transient. The measurement uncertainty is inversely proportional to the bunch charge, because the greater the charge, the greater the signal-to-noise ratio, so this is consistent with the theory. When the charge is about 600 pC, the bunch-by-bunch transverse position measurement uncertainty is better than 10 μm.

Similarly, we used the PCA method to evaluate the measurement uncertainty of the bunch-by-bunch longitudinal phase. It can be seen that the oscillation frequency and amplitude of each bunch are basically the same, but the initial phase is different. The longitudinal phase PCA decomposition results of the bunches are very concentrated. A mode with a singular value close to 1 occupies the largest

FIG. 16. The time domain waveforms of the first seven principal components in horizontal after the injection.
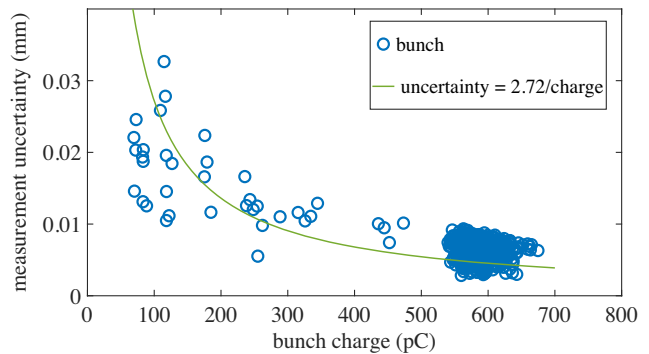

FIG. 18. The bunch-by-bunch transverse position measurement uncertainty with different bunch charge. The fitted line shows that the inverse relationship between the two is established.
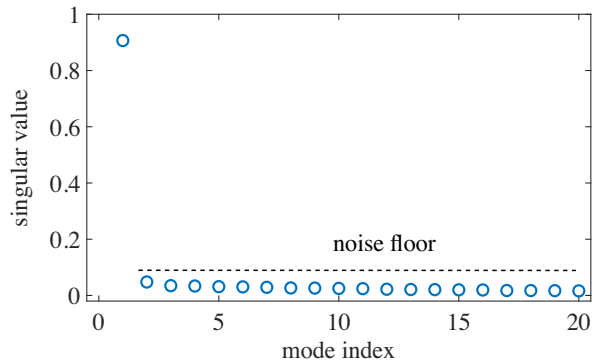
FIG. 19.   The singular values of each longitudinal phase mode obtained by PCA analysis.

FIG. 21.   The frequency spectrum analysis of the first principal components about longitudinal phase after the injection.

component of the longitudinal phase oscillation of the bunches (shown in Fig. 19).

The time-domain waveform (Fig. 20) and frequency spectrum (Fig. 21) of the first principal mode obtained by mode decomposition and Fourier transform are shown in the figure. It can be seen that the bunches in the storage ring have a strong common longitudinal oscillation. This oscillation is determined by the rf cavity and the longitudinal coupling wakefield.

After removing this mode, the rest is random measurement noise and undefinable high-order motion mode. The uncertainty of the longitudinal phase measurement is evaluated by the same method as the transverse position measurement. The measurement uncertainty of longitudinal phase is inversely proportional to the bunch charge. When the charge is about 600 pC, the bunch-by-bunch transverse position measurement uncertainty is better than 0.2 ps (shown in Fig. 22).

The sources of noise was evaluated. The main sources in the bunch-by-bunch measurement based on the high-sampling oscilloscope include two parts: One part is the clock jitter of the oscilloscope itself. The oscilloscope we use has a new generation of time reference structure which provides accurate time accuracy. The lowest internal clock jitter is less than 100 fs. Another part comes from the signal
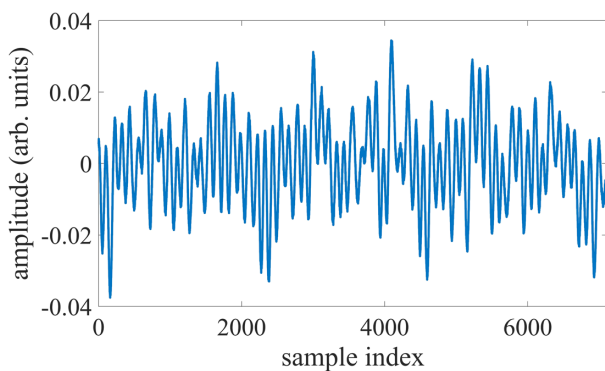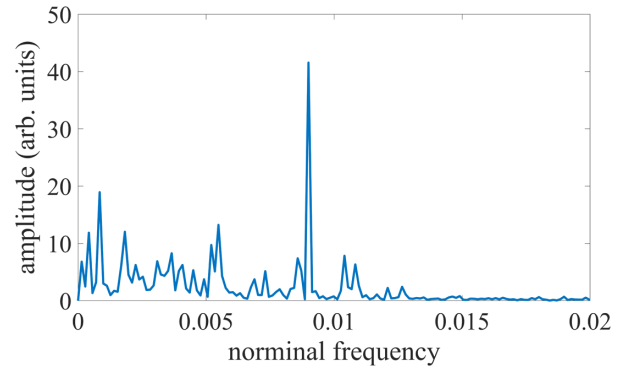
voltage measurement error(ADC effective bits). When the oscilloscope is in a dynamic range of plus or minus 5 V, the random measurement error of a single point is about 0.02 V. Different from other bunch-by-bunch measurement algorithms, our algorithm does not only use peak points but makes full use of all sampling points, so it has several times the processing gain.

The systematic error mainly comes from the crosstalk between bunches. According to Eqs. (10)–(13), this term was ignored as a constant. Because high-bandwidth acquisition equipment is used and the state of the bunches is stable, it is reasonable to ignore this item (Fig. 8 and Fig. 3). The mathematical analysis also support this point. If this item is not omitted, we find that the influence of it will be multiplied by $k - 1$ by rederive Eqs. (10)–(13). Because k is always close to 1, it has little effect. In fact, the crosstalk between bunches can be completely removed by iterating the current algorithm. The price of this is that it requires a lot of computing resources. In the future, we plan to evaluate the necessity of doing so.

The feasibility of this bunch-by-bunch information extraction algorithm on other devices has been study. Because the selected data acquisition equipment is an oscilloscope without an external clock. This means that

FIG. 20.   The time domain waveforms of the first principal components about longitudinal phase after the injection.
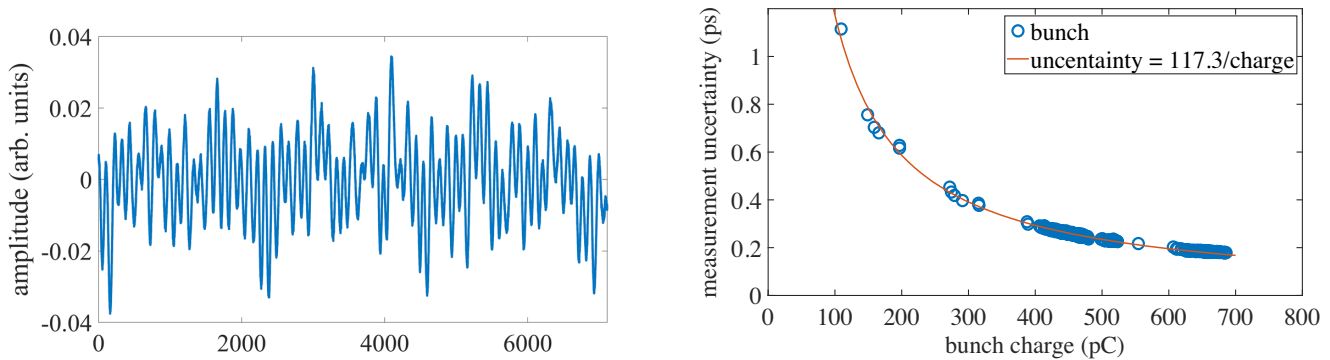

FIG. 22.   The bunch-by-bunch longitudinal phase measurement uncertainty with different bunch charge. The fitted line shows that the inverse relationship between the two is established.
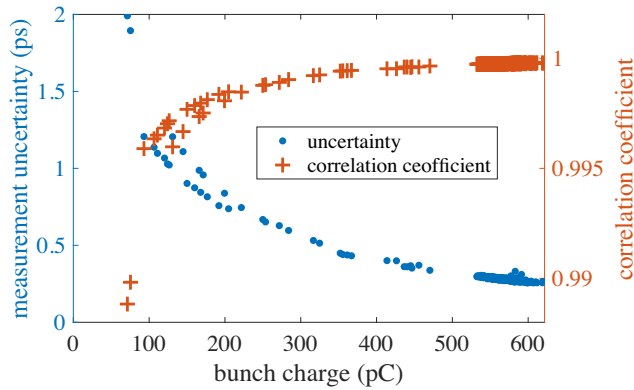
FIG. 23. The relationship between the measurement uncertainty and correlation_coefficient with different charge. Pearson correlation coefficient of measurement uncertainty and correlation_coefficient is about 0.95.

the measurement of the longitudinal phase is almost absolute (based on the timing system in the oscilloscope). However, the data acquisition phase and the bunch are not synchronized, which puts forward higher requirements on the extracting algorithm. We developed a vector-comparison-method based on correlation coefficient to solve it by comparing the data acquired every time when the bunch passes BPM with the response function of the bunch. correlation_coefficient represents the cosine of the angle between two vectors (bunch data and the response function). When correlation_coefficient is closer to 1, the two vectors are closer together. Therefore, correlation_coefficient can be used to characterize the error. The result of experiment is shown in Fig. 23.

In our experiment, the oscilloscope can capture 20 points when the bunch passes through the BPM each time. 10 of them are large enough to be effective. It can be seen from Fig. 5 that correlation_coefficient has the sharp peak around 1 with the different LUTs. When the sampling frequency of the oscilloscope is not high enough, the data will not be
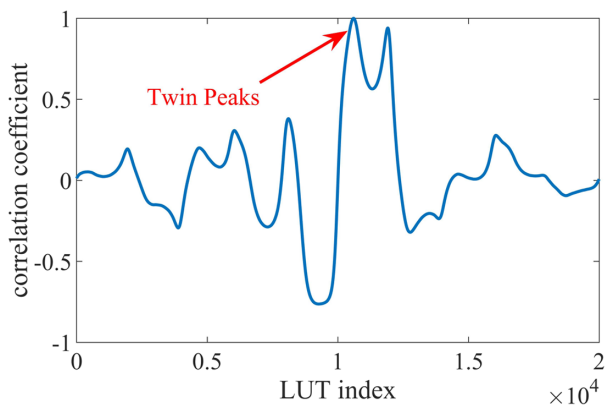

FIG. 24. The relationship between correlation_coefficient and index of LUT with 5 GHz sampling frequency (only 5 valid points).

enough to extract the phase. When the sampling frequency of the oscilloscope drops to 5 GHz, the number of effective points oscilloscope capture is 5 at a time. The result of correlation_coefficient in this case is shown in Fig. 24. It can be seen that at this time, the "1" peak of correlation_coefficient with different LUTs is not sharp, and even appears as double peaks. It is fatal to the vector-comparison-method which will cause larger measurement error, and even find a completely wrong matching result. According to our research, for a bipolar pulse signal, 8 or more data points are necessary.

VII. APPLICATION PROSPECTS

For BI engineers, comprehensive and multidimensional monitoring of beam state is the main goal. For physicists, single bunch is a basic unit for physics study. Parameters of individual bunch is more meaningful than average values. The bunch-by-bunch three-dimensional position and charge measurement system will be an important tool for physicists to study relativistic particles and high-energy physics. For example, during the injection transient, the fusion process of the injected bunch and the stored bunch can be observed with a high refresh rate. The system recommended in this paper has such capabilities. Therefore, a high repetition rate, accurate bunch-by-bunch three-dimensional position and charge measurement system has broad application prospects.

For 3D position and beam charge measurement, turn-by-turn transverse and longitudinal position can be obtained; combined with position measurement, position dependence of BPM sum signal can be evaluated, then the accuracy of beam charge monitor will be improved; for beam current measurement, refresh rate can reach to a few microseconds, which is far better than dc current transformer (DCCT), it is able to locate the occurrence of beam loss more accurately. In addition, there are some other accelerator parameters that can also be measured: the instantaneous rf frequency of the accelerator can be obtained while calculating the longitudinal phase, because the system works at the internal clock; beam orbit, dispersion function, chromaticity and other parameters can theoretically be calculated in real time [61,62]. In the future, we also plan to use machine learning algorithms to extract these parameters from the bunch-by-bunch information.

As a user facility, to provide more stable synchrotron radiation is the main task. Therefore, it is very important to find the cause of instability, The bunch-by-bunch three-dimensional position and charge measurement system provides the possibility of accurate three-dimensional correction of each bunch. Wakefield is one the main source [63–65]. For longitudinal wakefield measurement, by averaging the bunch-by-bunch longitudinal phase of each turn, the longitudinal equilibrium phase (acceleration phase to high frequency system) of each bunch can be obtained. By establishing a mathematical model, the longitudinal

wakefield function can be solved. This helps us optimize the filling pattern and reduce longitudinal instability. For transverse wakefield, the injection process is a good opportunity to calculate it. During injection, bunches will deviate from the equilibrium orbit with the action of kicker. Later, the transverse position oscillation is affected by the magnet and transverse wakefield. Therefore, we can calculate the transverse wakefield function with the bunch-by-bunch transverse position. Actually, establishing an in-situ wakefield extraction system based on bunch-by-bunch measurement is the next step SSRF BI group is committed to do. The injection process as another source of beam instability is the focus of research. Using the bunch-by-bunch measurement system, important parameters of the injection process can be measured by separating the response functions of the stored bunch and the injected bunch. We can use parameters to optimize the state of the injector to make the beam more stable. Using these parameters, the injector can be optimized to reduce beam instability. The bunch-by-bunch feedback system is the main tool to reduce beam instability and correct bunch deviation.

VIII. CONCLUSION

The bunch-by-bunch three-dimensional position and charge measurement has been completed at SSRF. With broadband oscilloscope which has high sampling rate, four channels and large memory capacity, the raw data of BPM signal was obtained. We have developed a set of algorithms based on correlation-coefficient to extract bunch-by-bunch information from the waveform. The measurement uncertainty of longitudinal phase is less than 0.2 ps, the uncertainty of transverse position is less than 10 μm and the charge uncertainty is 1.6 pC at 600 pC bunch charge in SSRF.

This is the first time to propose a technology that can continuously and synchronously measure the three-dimensional position and charge of all bunches in the storage ring on every turn. With unified hardware and processing software modules, the bunch-by-bunch processing system in this paper can synchronously output its three-dimensional position and charge each time the bunch passes through the BPM pick-up. For the longitudinal phase, the measurement uncertainty is reduced by one to two orders of magnitude compared with the existing methods. For the charge measurement, compared to the previous similar work, the measurement uncertainty is reduced to about one-third at the same repetition frequency. For the transverse position measurement, under the same conditions, the uncertainty of this system is not inferior to other common systems before.

This bunch-by-bunch measurement system can work in the regular operation mode of the synchrotron radiation accelerator, so as to realize the synchronous extraction of the parameters of each bunch. The feasibility of this bunch-by-bunch information extraction method on other devices has been studied. When the data acquisition equipment is suitable, this method is very versatile for various ring accelerators.

The bunch-by-bunch three-dimensional position and charge measurement system has broad application prospects. Next step, based on this, an in-situ wakefield extraction system is planned to be established. In addition, in order to optimize the injector, the bunch-by-bunch parameters during the injection process will be extracted. These studies will allow us to understand and optimize the beam instability.

As a price to improve accuracy, the algorithm of this system is more complicated than others and requires a lot of computing resources at the software level. For this reason, we tried to use the GPU as a part of the computing unit. In the future, we also plan to use machine learning algorithms to extract parameters from the bunch-by-bunch information.

[1] G. Yang, Y. Leng, R. Yuan, and Y. Yan, Beam instabilities based on spectrum of turn-by-turn position, High Power Laser Part. Beams **23**, 110842 (2011), http://www.hplpb.com.cn/en/article/id/5393.

[2] H. Tanaka *et al.*, Trends and challenges in the future storage ring light sources, in *Proc. of ICFA Advanced Beam Dynamics Workshop (FLS'18)* (JACoW, Geneva, 2018).

[3] Z. Duan *et al.*, Survey of injection schemes for next-generation light source rings, in *Proc. of ICFA Advanced Beam Dynamics Workshop (FLS'18)* (JACoW, Geneva, 2018).

[4] C. Steier, A. Allézy, A. Anders, K. Baptiste, E. Buice, K. Chow, G. Cutler, S. De Santis, R. Donahue, D. Filippetto *et al.*, Status of the conceptual design of als-u, in *9th Int. Particle Accelerator Conf.(IPAC'18), Vancouver, BC, Canada, April 29-May 4, 2018* (JACOW Publishing, Geneva, Switzerland, 2018), pp. 4134–4137.

[5] Y. Zhou, Z. Chen, B. Gao, N. Zhang, and Y. Leng, Bunch-by-bunch phase study of the transient state during injection, Nucl. Instrum. Methods Phys. Res., Sect. A **955**, 163273 (2020).

[6] Y. Wang and Z. Liu, Nsrl transformation of beam position monitoring system for electron storage ring and closed-track measurement, Journal of University of Science and Technology of China **28**, 732 (1998).

[7] P. Castro, Applications of the 1000-turns orbit measurement system at lep, in *Proceedings of the 1999 Particle*

Accelerator Conference (Cat. No.99CH36366), Vol. 1 (IEEE, New York, 1999), pp. 456–460, Vol. 1.

[8] H. Chen, J. Chen, B. Gao, and Y. Leng, Bunch-by-bunch beam size measurement during injection at Shanghai synchrotron radiation facility, Nucl. Sci. Tech. **29,** 79 (2018).

[9] G. Kotzian, D. Valuch, and W. Höfle, *Sensitivity of the LHC transverse feedback system to intra-bunch motion*, *Proceedings of IPAC2017, Copenhagen, Denmark* (JACoW, Geneva, Switzerland, 2017).

[10] G. Kotzian *et al.*, Transverse feedback parameter extraction from excitation data, in *8th Int. Particle Accelerator Conf.(IPAC'17), Copenhagen, Denmark, 14–19 May, 2017* (JACOW, Geneva, Switzerland, 2017), pp. 1920–1923.

[11] N. B. Kraljevic, P. Burrows, R. Ramjiawan, D. Bett, G. Christian, T. Bromwich, R. Bodenstein, and C. Perry, JACoW: Optimisation of a High-Resolution, Low-Latency Stripline Beam Position Monitor System for Use in Intra-Train Feedback, Tech. Rep. (2017).

[12] K. Scheidt and B. Joly, Upgrade of beam phase monitors for the esrf injector and storage ring, *Proceedings of IBIC2013, Oxford, UK,* 757 (2013), http://accelconf.web.cern.ch/IBIC2013/papers/wepc33.pdf.

[13] R. H. A. Farias, L. Lin, A. R. D. Rodrigues, P. F. Tavares, and A. Hofmann, Oscilloscope measurement of the synchronous phase shift in an electron storage ring, Phys. Rev. Accel. Beams **4,** 072801 (2001).

[14] T. Ieiri, K. Akai, H. Fukuma, T. Kawamoto, E. Kikutani, and M. Tobiyama, Bunch-by-bunch measurements of the betatron tune and the synchronous phase and their applications to beam dynamics at kekb, Phys. Rev. Accel. Beams **5,** 094402 (2002).

[15] Y. Yang, Y. Leng, Y. Yan, and N. Zhang, Bunch-by-bunch beam position and charge monitor based on broadband scope in ssrf, Proceedings of IPAC2013, Shanghai, China (2013), pp. 595–597, http://accelconf.web.cern.ch/IPAC2013/papers/mopme054.pdf.

[16] Y. Yang, Y.-B. Leng, Y.-B. Yan, and Z.-C. Chen, Injection performance evaluation for SSRF storage ring, Chin. Phys. C **39,** 097003 (2015).

[17] L. Duan, Y. Leng, R. Yuan, and Z. Chen, Injection transient study using a two-frequency bunch length measurement system at the SSRF, Nucl. Sci. Tech. **28,** 93 (2017).

[18] Z. Chen, Y. Yang, Y. Leng, and R. Yuan, Wakefield measurement using principal component analysis on bunch-by-bunch information during transient state of injection in a storage ring, Phys. Rev. Accel. Beams **17,** 112803 (2014).

[19] H. Chen, J. Chen, B. Gao, L. Lai, Y. Leng, and N. Zhang, A fast beam size diagnostic system using high-speed photomultiplier array at ssrf, in *8th Int. Particle Accelerator Conf.(IPAC'17), Copenhagen, Denmark, 14–19 May, 2017* (JACOW, Geneva, Switzerland, 2017), pp. 345–348.

[20] Y. Zhou, H. Chen, S. Cao, and Y. Leng, Bunch-by-bunch longitudinal phase monitor at SSRF, Nucl. Sci. Tech. **29,** 113 (2018).

[21] X. Xu, Y. Leng, and Y. Zhou, Machine learning application in bunch longitudinal phase measurement, in *Proceedings of the 10th International Particle Accelerator Conference* (JACOW, Melbourne, Australia, 2019), pp. 2625–2628.

[22] X. Xu, Y. Zhou, and Y. Leng, Machine learning based image processing technology application in bunch longitudinal phase information extraction, Phys. Rev. Accel. Beams **23,** 032805 (2020).

[23] K. K. T. Nakamura, S. Dat, and T. Ohshima, Transverse bunch-by-bunch feedback system for the spring-8 storage ring, in *Proceedings of the 9th European Particle Accelerator Conference, Lucerne, 2004* (EPS-AG, Lucerne, 2004) [http://accelconf.web.cern.ch/AccelConf/e04/].

[24] V. Poucki, P. Lemut, M. Oblak, and T. Karcnik, Combating multibunch instabilities with the libera bunch-by-bunch unit, in *Proceedings of the 11th European Particle Accelerator Conference, Genoa, 2008* (EPS-AG, Genoa, Italy, 2008), p. 1251–1253.

[25] D. Teytelman, igp-120f signal processor-technical user manual, Dimtel Inc (2008).

[26] W. Barry, J. Byrd, J. Corlett, J. Johnson, G. Lambertson, and J. Fox, Commissioning of the als transverse coupled-bunch feedback system, in *Proceedings Particle Accelerator Conference* (IEEE, New York, 1995), Vol. 4, pp. 2423–2425.

[27] W. Barry, J. Byrd, J. Corlett, M. Fahmie, J. Johnson, G. Lambertson, M. Nyman, J. Fox, and D. Teytelman, Design of the pep-ii transverse coupled-bunch feedback system, in *Proceedings Particle Accelerator Conference* (IEEE, New York, 1995), Vol. 4, pp. 2681–2683.

[28] A. Drago, J. Fox, D. Teytelman, and M. Tobiyama, Commissioning of the igp feedback system at daϕne, SLAC National Accelerator Laboratory (United States). Funding organisation: US Department of Energy (United States) (2011).

[29] M. Höner, A. Nowaczyk, M. Bakr, H. Huck, S. Khan, R. Molo, A. Schick, P. Ungelenk, and M. Zeinalzadeh, Bunch-by-bunch feedback systems at the delta storage ring, in *Proc. 3rd Int. Particle Accelerator Conf* (JACoW, Geneva, 2012).

[30] C. Kuo, K. Hu, Y. Cheng, P. Chiu, Y. Chen, and K. Hsu, New bunch-by-bunch feedback system for the tls, in *Proceedings of DIPAC2011, Hamburg, Germany* (1995), http://accelconf.web.cern.ch/DIPAC2011/papers/tupd23.pdf.

[31] Operational status of the transverse multibunch feedback system at diamond.

[32] E. Huttel, N. Hiller, V. Judin, B. Kehrer, S. Marsching, A. Müller, and N. Smale, Characterization and stabilization of multi-bunch instabilities at the anka storage ring, in *3rd Int. Particle Accelerator Conf.(IPAC'12), New Orleans, Louisiana, USA* (JACoW, Geneva, 2012).

[33] L. M. Y. F. S. L. W. J. Yue, J. S. Cao, and X. Y. Zhao, Longitudinal and transverse feedback systems for the bepcii storage rings, in *Proceedings of IBIC2013, Oxford, UK* (2013), pp. 373–375, http://accelconf.web.cern.ch/IBIC2013/papers/tupc09.pdf.

[34] W. Li, Development of digital bunch-by-bunch feedback system for storage ring HLS II, Ph.D. thesis, USTC (2014).

[35] J. Lee, M. H. Chun, G.-J. Kim, D.-C. Shin, D.-T. Kim, and S. Shin, Bunch-by-bunch position measurement and analysis at PLS-II, J. Synchrotron Radiat. **24,** 163 (2017).

[36] S. Prabhakar, R. Claus, J. Fox, H. Hindi, I. Linscott, J. Olsen, W. Ross, and D. Teytelman, Observation and modal analysis of coupled-bunch longitudinal instabilities via a digital feedback control system, Part. Accel. **390,** 207 (1997).

[37] D. Teytelman, C. Rivetta, D. Van Winkle, R. Akre, J. Fox, A. Krasnykh, and A. Drago, Design and Testing of Gproto Bunch-by-bunch Signal Processor, Conf. Proc. C **060626,** 3038 (2006).

[38] D. Teytelman, J. Fox, W. Cheng, J. Flanagan, T. Naito, M. Tobiyama, and A. Drago, Control and measurements of longitudinal coupled-bunch instabilities in the ATF damping ring, Proceedings of PAC07, Albuquerque, New Mexico, USA (2007), p. 584.

[39] W. K. Lau, S. J. Lin, M. S. Yeh, L. H. Chang, T. T. Yang, K. T. Hsu, M. H. Wang, and C. C. Kuo, Development of a digital longitudinal damper for the tls storage ring, in *Proceedings of the 1997 Particle Accelerator Conference (Cat. No. 97CH36167)* (IEEE, New York, 1997), Vol. 2, pp. 2377–2379.

[40] R. H. A. Farias, L. Lin, A. R. D. Rodrigues, P. F. Tavares, and A. Hofmann, Oscilloscope measurement of the synchronous phase shift in an electron storage ring, Phys. Rev. Accel. Beams **4,** 072801 (2001).

[41] W. Cheng, B. Bacha, K. Ha, and O. Singh, Precise synchronous phase measurements, in *Proc. of International Particle Accelerator Conference (IPAC'17), Copenhagen, Denmark, May, 2017*, International Particle Accelerator Conference No. 8 (JACoW, Geneva, Switzerland, 2017), pp. 487–490.

[42] T. Ohshima, A. Yamashita, and M. Yoshioka, Beam phase measurement of stored bunch, in *Proceedings of the 10th European Particle Accelerator Conference, Edinburgh, Scotland, 2006* (EPS-AG, Edinburgh, Scotland, 2006), p. 1133.

[43] Y. Kobayashi and M. Izawa, A longitudinal phase space monitor at the photon factory storage ring, in *Proceedings of the 1997 Particle Accelerator Conference (Cat. No. 97CH36167)* (IEEE, New York, 1997), Vol. 2, pp. 2171–2173.

[44] T. Ieiri and T. Kawamoto, A four-dimensional beam-position monitor, Nucl. Instrum. Methods Phys. Res., Sect. A **440,** 330 (2000).

[45] T. Ieiri, K. Akai, H. Fukuma, and M. Tobiyama, Beam dynamics measurements using a gated beam-position monitor at kekb, Nucl. Instrum. Methods Phys. Res., Sect. A **606,** 248 (2009).

[46] C. Zhichu, L. Yongbin, Z. Yi, Y. Yingbin, and Z. Weimin, Baseline recovery method to measure bunch charge under low-current mode of ssrf, Nucl. Sci. Tech. **22,** 264 (2013).

[47] Y. Q. D. Qingyong and C. Jianshe, Bunch current measurement system for bepc-ii storage ring, High Power Laser Part. Beams **26,** 75101 (2014).

[48] F. Chen, L. Lai, Y. Leng, Y. Yan *et al.*, Design of a new type of beam charge monitor based on bunch by bunch daq system, in *6th Int. Beam Instrumentation Conf.(IBIC'17), Grand Rapids, MI, USA, 20-24 August 2017* (JACOW, Geneva, Switzerland, 2018), pp. 284–286.

[49] S. D. Santis, D. Li, W. Norum, and G. Portmann, Bunch charge monitor for the als upgrade, Proceedings of the 7th Int. Beam Instrumentation Conf. (IBIC'18), Shanghai, China, 2018, paper MOOC04 (unpublished).

[50] D. Peake, M. Boland, G. LeBlanc, and R. Rassool, Measurement of the real time fill-pattern at the australian synchrotron, Nucl. Instrum. Methods Phys. Res., Sect. A **589,** 143 (2008).

[51] B. Kalantari, V. Schlott, and T. Korhonen, Bunch pattern control in top-up mode at the swiss light source, in *Proceedings of the 9th European Particle Accelerator Conference, Lucerne, 2004* (EPS-AG, Lucerne, 2004), p. 2885 [http://accelconf.web.cern.ch/AccelConf/e04/].

[52] T. Zhou, Y. Yang, B. Sun, P. Lu, F. Wu, J. Wang, Z. Zhou, Q. Luo, Q. Wang, and H. Li, Bunch current measurement using a high-speed photodetector at hls ii, IEEE Trans. Nucl. Sci. **64,** 1886 (2017).

[53] R. E. Shafer, Beam position monitoring, AIP Conf. Proc. **249,** 601 (1992), https://aip.scitation.org/doi/pdf/10.1063/1.41980.

[54] S. R. Smith, Beam position monitor engineering, AIP Conf. Proc. **390,** 50 (1997).

[55] G. Wang *et al.*, Beam diagnostics using bpm signals from injected and stored beams in a storage ring, Proceedings of 2011 Particle Accelerator Conference (IPAC2011), New York, NY, USA (2011).

[56] W. Cheng, B. Bacha, B. Kosciuk, O. Singh, and S. Krinsky, Performance of nsls2 button bpms, *Proceedings of IBIC2013, Oxford, UK* (2013), http://accelconf.web.cern.ch/IBIC2013/papers/wepc33.pdf.

[57] J. Irwin, C. X. Wang, Y. T. Yan, K. L. F. Bane, Y. Cai, F.-J. Decker, M. G. Minty, G. V. Stupakov, and F. Zimmermann, Model-Independent Beam Dynamics Analysis, Phys. Rev. Lett. **82,** 1684 (1999).

[58] C. x. Wang, Measurement and application of betatron modes with mia, in *Proceedings of the 2003 Particle Accelerator Conference* (IEEE, New York, 2003), Vol. 5, pp. 3407–3409.

[59] Y. R. Chen Z and Leng Y, Beam position monitor troubleshooting by using principal component analysis in shanghai synchrotron radiation facility, Nucl. Sci. Tech. **25** (2014), .

[60] Y. R. Y. Y. Z. W. C. Zhichu and L. Yongbin, Study of algorithms of phase advance measurement between bpms and its application in ssrf, Nucl. Sci. Tech. **24,** 010102 (2013).

[61] K. Oide *et al.*, Design of beam optics for the future circular collider e^+e^- collider rings, Phys. Rev. Accel. Beams **19,** 111005 (2016).

[62] H. Hotchi, N. Tani, Y. Watanabe, H. Harada, S. Kato, K. Okabe, P. K. Saha, F. Tamura, and M. Yoshimoto, Beam loss caused by edge focusing of injection bump magnets and its mitigation in the 3-gev rapid cycling synchrotron of the japan proton accelerator research complex, Phys. Rev. Accel. Beams **19,** 010401 (2016).

[63] R. Nagaoka, Instability studies using evaluated wake fields and comparison with observations at soleil, in *Proceedings of the 10th European Particle Accelerator Conference,*

Edinburgh, Scotland, 2006 (EPS-AG, Edinburgh, Scotland, 2006), pp. 2847–2849.

[64] F. J. Cullinan, R. Nagaoka, G. Skripka, and P. F. Tavares, Transverse coupled-bunch instability thresholds in the presence of a harmonic-cavity-flattened rf potential, Phys. Rev. Accel. Beams **19,** 124401 (2016).

[65] A. Lasheen, T. Argyropoulos, T. Bohl, J. F. E. Müller, H. Timko, and E. Shaposhnikova, Beam measurement of the high frequency impedance sources with long bunches in the cern super proton synchrotron, Phys. Rev. Accel. Beams **21,** 034401 (2018).